Asia-Pacific J. Atmos. Sci., 47(3), 245-253, 2011
DOI:10.1007/s13143-011-0013-z

Representation of Tropical Storms in the Northwestern Pacific by the Modern-Era Retrospective Analysis for Research and Applications

Myong-In Lee[1], Siegfried D. Schubert[2] and Dongmin Kim[1]

[1]*Ulsan National Institute of Science and Technology, Ulsan, Korea*
[2]*NASA Goddard Space Flight Center, Greenbelt, MD, U. S. A.*

(Manuscript received 25 December 2010; revised 13 January 2011; accepted 15 January 2011)

Abstract: This study examines the tropical storms simulated in the Modern-Era Retrospective analysis for Research and Applications (MERRA) global atmospheric reanalysis for the recent 12 years (1998-2009), focusing on the tropical storm activity over the Northwestern Pacific. For validation, the International Best Track Archive for Climate Stewardship (IBTrACS) dataset is used as an observational counterpart. Climatological-mean features of the tropical storm genesis, tracks and their maximum intensity are the primary interests in this study. Regarding the genesis location of tropical storms, MERRA is reasonable in resolving major development regions over the South China Sea and the Northwestern Pacific close to the Philippines. The seasonal variation of the number of storms is also reproduced in a realistic way in MERRA, with peak values occurring from July to September. In addition, MERRA tends to reproduce the observed interannual variation of the number of tropical storms during the 12-years, though with a limited accuracy. The simulated paths toward higher latitudes are also reasonable in MERRA, where the reanalysis corresponds well with the observations in resolving frequent paths of westward moving storms and recurving storms toward the northeast. Regarding the intensity, MERRA captures the linear relationship between the minimum center pressure and the maximum wind speed near the surface at the maximum development. Some discrepancies from the observed features are found in the reanalysis, such as less frequent development of storms over the South China Sea and less frequent paths over this region. The reanalysis also does not attain the observed maximum intensity for the resolved tropical storms, particularly underestimating the center pressure. These deficiencies are likely related to limitations in the horizontal resolution and the parameterized physics of the data assimilation system.

Key words: Tropical storms, Northwestern Pacific, atmospheric reanalysis, data assimilation

1. Introduction

Atmospheric reanalyses have been an important resource for studying weather, climate, and its variability. Reanalyses are produced by a data assimilation system that blends the output of a numerical model with vast quantities of observational data, and provide a coherent and physically-consistent representation of atmospheric states from observations that are incomplete in both space and time. Over the last two decades there have been continuous efforts in developing and improving global reanalysis products (e.g., Kalnay *et al*., 1996; Kanamitsu *et al.*, 2002; Uppala *et al*., 2005; Onogi *et al*., 2007; Saha *et al*., 2010). Substantial advances have been made in Earth observing networks, data assimilation techniques, and global numerical models - key components of a data assimilation system. These products are being used in many operational and research applications, for example, by providing initial and boundary conditions for global and limited-domain weather, climate, and hydrological forecast models.

With the continuous evolution of data assimilation systems, the quality of reanalyses have improved substantially, and the range of potential applications has increased. In addition to providing better quality data that are more consistent with observations, modern reanalyses are providing more detailed data with finer spatial resolution and higher temporal frequency (e.g., 1-hour products). This enables the investigation of extreme weather events such as the development of mesoscale convective systems and tropical storms. The capability of resolving these extreme weather events in a high-resolution data assimilation product is invaluable in many scientific studies and other potential applications.

The National Aeronautics and Space Agency (NASA) recently released a new, global reanalysis, named the Modern-Era Retrospective analysis for Research and Applications (MERRA, Rienecker *et al.,* 2011). The reanalysis utilized the Goddard Earth Observing System version 5 (GEOS-5, Rienecker *et al.,* 2008) global data assimilation system to synthesize the various in-situ and satellite observations for the period 1979-present. Special emphasis was placed on improving estimates of the hydrological cycle on a broad range of weather and climate time scales (Bosilovich *et al.,* 2008). The MERRA dataset has several advances that facilitate research and applications. First, the atmospheric general circulation model used in the data assimilation system has a higher spatial resolution (1/2° latitude × 2/3° longitude with 72 vertical levels extending to 0.01 hPa), compared with earlier reanalyses. Also, two dimensional diagnostics such as precipitation, surface fluxes and single level meteorology are provided at 1 hour intervals including coarser (1.25° × 1.25°) resolution products, as well as traditional 6-hourly atmospheric analyses at the native spatial resolution (1/2° × 2/3°). These high-resolution products provide an opportunity for diagnosing high-impact weather extremes such as tropical storms.

Accurate seasonal predictions of the genesis, number, intensity,

Corresponding Author: Dr. Myong-In Lee, School of Urban and Environmental Engineering, Ulsan National Institute of Science and Technology, 100 Banyeon-ri, Ulju-gun, Ulsan 689-798, Korea.
E-mail: milee@unist.ac.kr

and the most probable tracks of tropical storms are indispensible information in preparing for and minimizing damages caused by this high-impact natural disaster, although predictions based on numerical forecast systems have been less reliable so far, compared with statistical forecast schemes. A careful investigation of reanalyses regarding their ability to represent extreme weather events such as tropical storms has at least two important scientific implications. First, from the point of achieving reliable budgets of global energy and water cycles, this must include a reasonable reproduction of these high-frequency weather extremes (Bosilovich *et al.,* 2011). Second, the validation of tropical storms in the reanalysis is useful in exploring the untapped dynamic predictability of such phenomena. Although being continuously influenced by observations during the assimilation cycle, the MERRA assimilation system did not use a tropical storm relocator or the artificial bogusing of storms. This allows for a useful validation on how the model responds to the large-scale forcing that might trigger and sustain tropical storms. MERRA is useful in this case, where the hurricane-like vortices are reasonably simulated with axially symmetric wind structure, with warm core at the center driven by subsidence at 50 km horizontal resolution or higher. The response of the model is largely a function of grid spacing and the parameterized physics, particularly the deep convection scheme, whilst the horizontal resolution of 50 km is not yet fine enough to capture the details of tropical storms. Examinations of the degree to which the model represents the structure, intensity, and the migration paths will provide useful information to validate and improve the tropical storm simulations for the given resolution.

This study examines the representation of tropical storms in MERRA for the recent 12 years (1998-2009). For validation, the International Best Track Archive for Climate Stewardship (IBTrACS) dataset for the same time period is used. Our investigation is limited to the tropical storms formed over the Northwestern Pacific. The typhoon is a tropical storm that develops in the northwestern part of the Pacific Ocean between 100° and 180°E, and is one of the most devastating weather events in East Asia. The typhoons continuously develop through out the year, although they exhibit a strong seasonal variation such that the majority of storms form between May and December whilst tropical cyclone formation is at a minimum between January and April. The number of tropical storms developed over the Northwestern Pacific also changes year by year with about 20 storms per year on average. We specifically focus on the quantitative validation of the climatological features of the tropical storm genesis, frequent paths and their maximum intensity, and examine whether these observed features are reasonably reproduced in the reanalysis.

2. Data and methods

a. Data

We evaluate the representation of tropical storms for the most recent 12 years (1998-2009) simulated in the MERRA reanalysis. MERRA is a state-of-the-art atmospheric reanalysis produced by the high-resolution (1/2° latitude × 2/3° longitude, 72 vertical levels) GEOS-5 data assimilation system developed by NASA. The MERRA products begin in 1979 to the present covering the modern era of remotely sensed data from various satellites. For the details on the data assimilation system, the data production procedures, and the selected results for weather and climate diagnostics, refer to Rienecker *et al*. (2011) and the MERRA special papers referenced therein. Here we briefly introduce MERRA.

The GEOS-5 atmospheric general circulation model used for MERRA is based on a finite-volume dynamical core developed by Lin (2004). The model includes parameterized physics of short-wave (Chou and Suarez, 1999) and long-wave radiation (Chou *et al.,* 2001), cumulus convection (Moorthi and Suarez, 1992), cloud process (Bacmeister *et al.,* 2006), boundary-layer turbulence (Louis *et al.,* 1982; Lock *et al.,* 2000), land surface processes (Koster *et al.,* 2000), and gravity wave drag (McFarlane, 1987; Garcia and Boville, 1994), which have been modified and tuned from the original parameterization schemes.

For the analysis algorithm, MERRA uses a three-dimensional variational method (3D-Var) based on the Grid-point Statistical Interpolation scheme (GSI, Wu *et al.,* 2002). During the data assimilation cycle starting every six hours, the analysis correction is applied to the global model by adding the correction tendency term (the GSI analysis minus the model forecast) in the model equations. This tendency term is gradually inserted into the model in order to slowly adjust the model state toward the observed state during the assimilation cycle, based on the incremental analysis update (IAU) method described by Bloom *et al.* (1996).

Various types of observational data are used for MERRA, including both conventional observations and satellite radiance data (for the complete list of input data, see Appendix A in Rienecker *et al.,* 2011). Conventional observations include the routine measurements of standard atmospheric variables (i.e., pressure, temperature, height, winds) taken from the weather stations, balloons, aircraft, ships, and buoy. Satellite observations are also extensively used for MERRA, according to their availability. Notable additions to the data stream in recent years include the cloud-track winds from the Moderate Resolution Imaging Spectroradiometer (MODIS, 2002-present), surface wind speed over the ocean from the Special Sensor Microwave/Imager (SSM/I, 1987-present) and the Quick Scatterometer (QuickScat, 1999-present) and temperature- and humidity-sensitive infrared radiance from the Advance Infrared Sounders (AIRS).

Although the MERRA reanalysis provides the data over the whole globe, we focus on the northwest Pacific basin (100-180°E, 0-50°N), which exhibits the largest formation of tropical storms and typhoons. We sampled the atmospheric wind and temperature data in every three hour from the hourly products at the condensed resolution (1.25° × 1.25°) in order to track simulated tropical storms more accurately in time. Although MERRA provides 6-hourly native resolution outputs at 1/2° latitude by 2/3° longitude, these are only available for selected

variables at 200, 500, and 850 hPa, which are not enough to apply the tropical storm detection and tracking algorithm used in this study. We note that the use of condensed resolution output might decrease the maximum intensity of the resolved storms, and is less ideal than to use the native resolution outputs at half degree. However, it is not expected to substantially alter the climatological features of the tropical storms such as the genesis number, locations, and tracks of the storms, which is our primary interest here. For convenience, we re-gridded the output to $1^o \times 1^o$ horizontal resolution for the selected variables-sea level pressure, atmospheric winds at 200, 850, and 925 hPa, 10-m surface wind, and temperatures at 300, 500, and 700 hPa - that required by the tropical storm detection and tracking algorithm.

For the comparison, we analyzed the observed IBTrACS data (Knapp *et al.,* 2010) provided by the U.S. National Center for Climate Data (NCDC). The IBTrACS is a recently-released, global best track dataset of tropical storms produced by merging various tropical storm reports from multiple centers into one product. Therefore, the results from this study are expected to be consistent with existing studies from the observations (Knapp *et al.,* 2010). As the observation shows a strong seasonal variation in the tropical storm activity over the northwest Pacific basin, we limit our analysis to the active tropical storm season from 1 April to 30 November. In the analysis, we excluded the storms not exceeding 35 knots in the surface wind speed at its maximum development. These storms are classified as a tropical depression, which is the lowest category based on the Japan Meteorological Agency (JMA)'s Regional Specialized Meteorological Center (RSMC) classification. Surface wind speed is not available for this category in IBTrACS.

b. Methods

The detection and tracking algorithm of simulated tropical storms is based on the method originally developed by Camargo and Zebiak (2002), and further modified by the National Center for Environmental Prediction (NCEP) Climate Prediction Center (CPC). The detection algorithm relies on the threshold criteria for three atmospheric variables, including the relative vorticity at 850 hPa ($\zeta_{threshold}$), the wind speed at 10 m above the surface ($|v|_{threshold}$), and the vertically-integrated temperature anomaly at the storm center ($[T]_{threshold}$). The last condition is intended to detect the warm-core structure of well-defined tropical storms induced by subsidence heating at the core. As these quantities are dependent on the models and geographical locations, the method first calculates the standard deviation of each variable using the data of the entire analysis period. Then, the three threshold values are defined for each variable and each basin (here we just consider the northwest Pacific basin). For practical reasons, we integrated the temperature anomalies at three pressure levels of 300, 500, and 700 hPa to represent the vertically-integrated temperature anomaly. As in Camargo and Zebiak, we chose $\zeta_{threshold} = 3.26 \times 10^{-5}$ s^{-1}, $|v|_{threshold} = 3.45$ m s^{-1}, $[T]_{threshold} = 0.46$ K, which is 2 times the standard deviation of the 850-hPa vorticity, the global average and the one standard deviation of the 10-m wind speed in the basin, and one standard deviation of the vertically-integrated temperature anomaly, respectively. These are basin-specific values. Once the detection algorithm finds the point of the tropical storm that meet the three criteria simultaneously, the storm is tracked forward and backward in time to construct a full storm track and ensure the storm is not counted more than once. We also use an additional criterion based on the duration (lifetime) of the detected tropical storm. In particular, storms that lived less than a day in the reanalysis are discarded in this study, which is quite rare in the observational cases.

The threshold values in the Camargo-Zebiak algorithm are model-dependent, and subject to adjustments according to the simulated variance statistics. For example, they use a one standard deviation threshold for the vertically-integrated temperature anomaly, whereas the 0.5 standard deviation is used in the modified algorithm by CPC for the validation of the NCEP Climate Forecast System (CFS) model (L. Williams, personal communication). In our sensitivity tests, the change in threshold value from 1 to 0.5 standard deviations does not lead to significant changes in the simulated tropical storm climatology in a qualitative sense (i.e., the spatial distribution of genesis, track, seasonal and interannual variation of storm numbers), although the decrease of the threshold values does increase the total number of storms by about 25% from the 1 standard deviation case. The total number of storms detected by the one standard deviation threshold is 252 for 12 years, which is very close to the observed number of 251. The reanalysis is correlated slightly better with the observational data in terms of the interannual variation of the tropical storm number in the 0.5 standard deviation case (0.65), compared with the 1 standard deviation case (0.59), but this seems to be a marginal improvement for the given samples.

3. Results

a. Validation for selected storms

Before we go into the validation of the long-term statistics of tropical storms simulated by MERRA, we selected a few individual storm cases and examined the track and the intensity changes in time. This validation is useful to understand the basic characteristics of the simulated storms in the reanalysis. Two tropical storms are selected and presented in Fig. 1, highlighting some typical cases in MERRA. For the case of Typhoon Ewiniar (2006), MERRA follows the observed track reasonably well in the initiation and migration toward the extra-tropics until the time of landfall at the Korean peninsula. After landfall the typhoon decreased its intensity and changed into an extra-tropical low-pressure system, and thereafter the tracking error becomes larger. The observations and the reanalysis show some discrepancy in the intensity at the maximum development. Ewiniar had a minimum sea level pressure of 930 hPa with a maximum sustained 10-m wind speed of 100 knots at 1800 UTC 4 July. On the other hand, the MERRA storm had a minimum sea level pressure of 990 hPa at its maximum development

phase, and this occurred about 4 days later than observed. The instantaneous wind speed at 925 hPa level, which is a substitute for the surface wind in the reanalysis in this study, reaches a value close to 70 knots. It is interesting to see that there exist sub-daily variations in the simulated time series of sea level pressure and wind speed at the storm center. A distinct cycle with a 6-hour period, particularly in the sea level pressure, is likely related to the 6 hour updates associated with the analysis cycle. Diurnal variations are also noticeable in the simulated time series - a feature that is not clearly evident in the IBTrACS tropical storm observations.

The simulation of Typhoon Jangmi (2008) is one of the best cases in MERRA in terms of its formation and migration. The reanalysis captures the observed developing location in the tropical Western Pacific, and then the simulated track follows the observed track toward the northwest until the storm hit Taiwan. After landfall, the observed typhoon moved northeast and then retreated toward the tropics, which is simulated reasonably well by MERRA. Although the minimum center pressure remains around 987 hPa in the reanalysis, compared with the observed deepening of about 900 hPa, the timing of the maximum development is relatively accurate within a day difference between the reanalysis and the observation.

Based on the discussion above, MERRA shows some defects in the representation of individual tropical storms. The reanalysis has some difficulty in reproducing the correct temporal variation of the intensity change, as well as the observed peak intensity. Another characteristic is a general tendency of earlier detection of the storm than observed (as illustrated in Figs. 1c and 1d), which is likely related to the tropical storm detection algorithm (this will be revisited in the next section). Therefore, the diagnostics for individual storms, such as the intensity change in time, may not be realistic. Nevertheless, considering the relatively accurate storm tracks in MERRA as exemplified by Fig. 1, it should be meaningful to validate the long-term averaged statistics to describe the tropical storm climatology in MERRA. This will be elaborated in the following sections.

b. Tropical storm genesis

We first compare the genesis location of tropical storms that developed during April to November for the past 12 years (1998-2009) between IBTrACS and MERRA (Fig. 2). Genesis points of the observed tropical storms are widely spread over

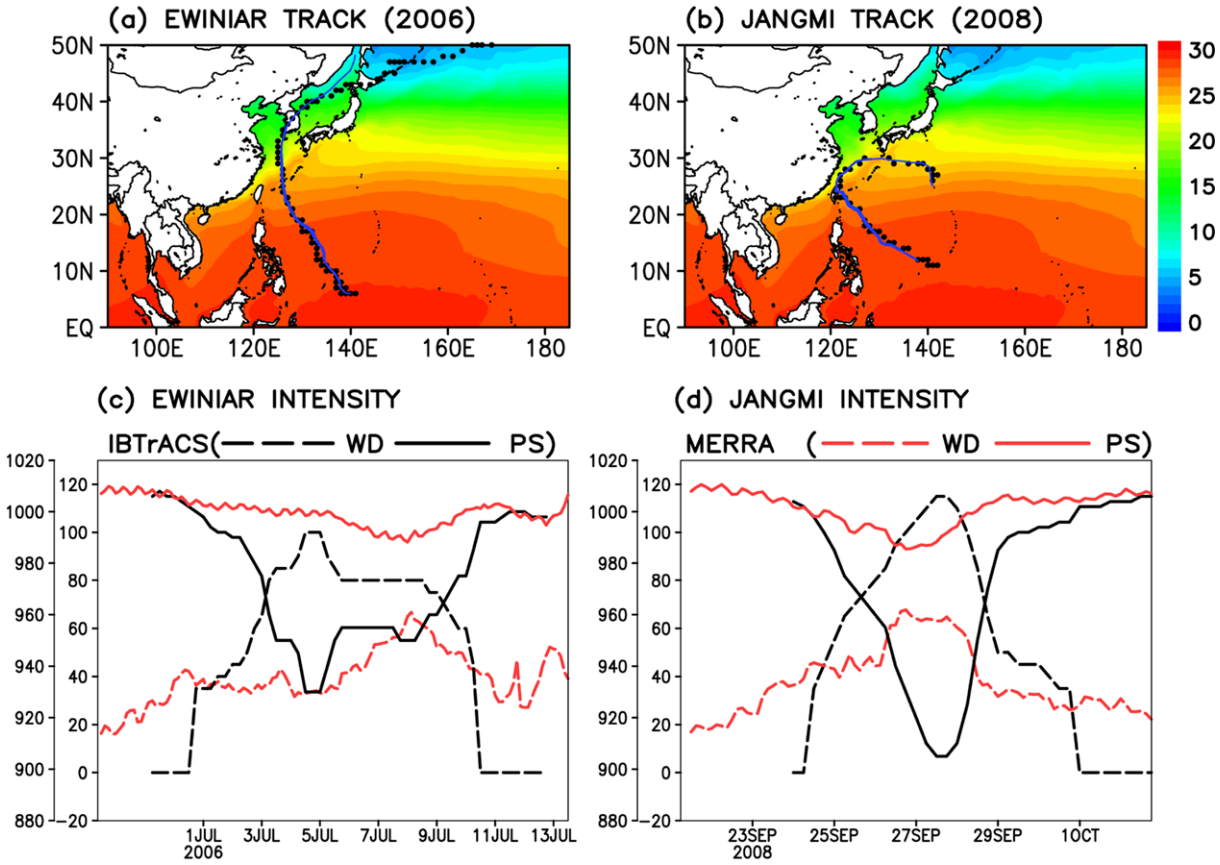

Fig. 1. Comparison of the tropical storm track and the intensity for the two selected cases of Typhoon Ewiniar (2006, left) and Typhoon Jangmi (2008, right). (a) and (b) compare the storm tracks between the IBTrACS observation (solid blue line) and the MERRA reanalysis (filled circles). Shaded is the annual-mean sea surface temperature (SST) climatology averaged for 1998-2009, which was obtained from the National Oceanic and Atmospheric Administration (NOAA) Optimum Interpolation 1/4 degree daily SST analysis. (c) and (d) compare the temporal changes of the sea level pressure (solid line, unit: hPa) and the surface wind speed (dashed line, unit: knots) at the storm center from IBTrACS (black) and MERRA (red).

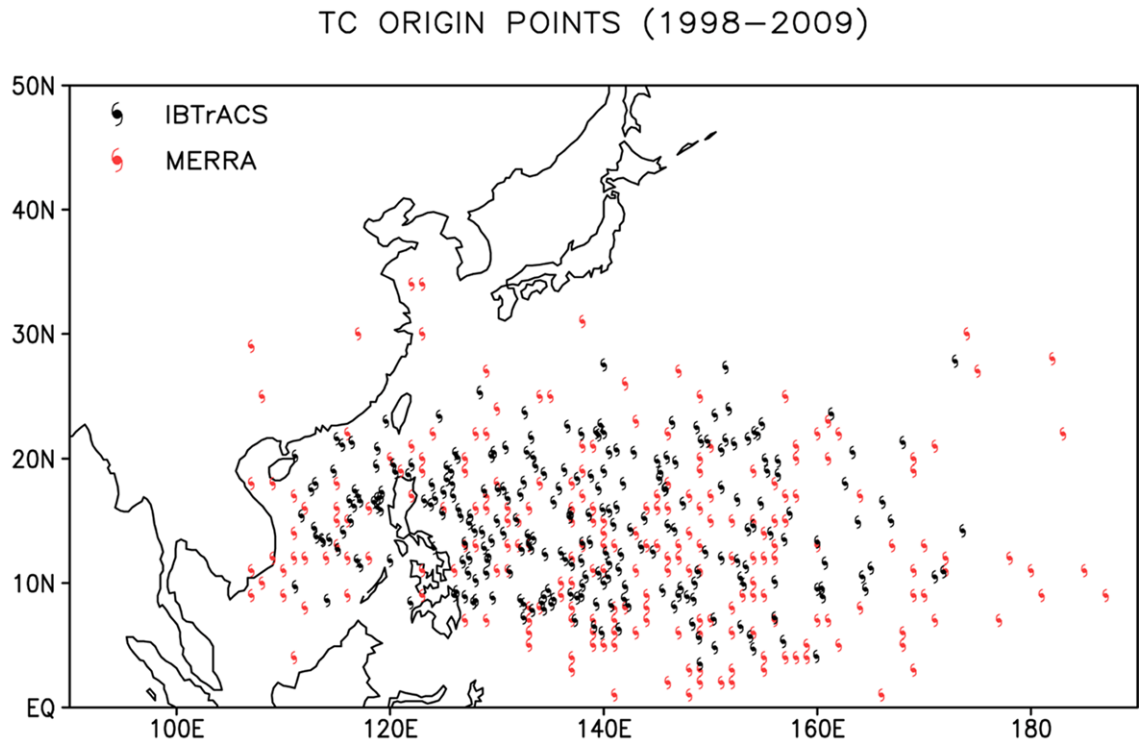

Fig. 2. Genesis points of tropical storms in IBTrACS (black) and MERRA (red). Only compared are the tropical storms generated during April to November 1998-2009. Values represent the total storm number generated per decade.

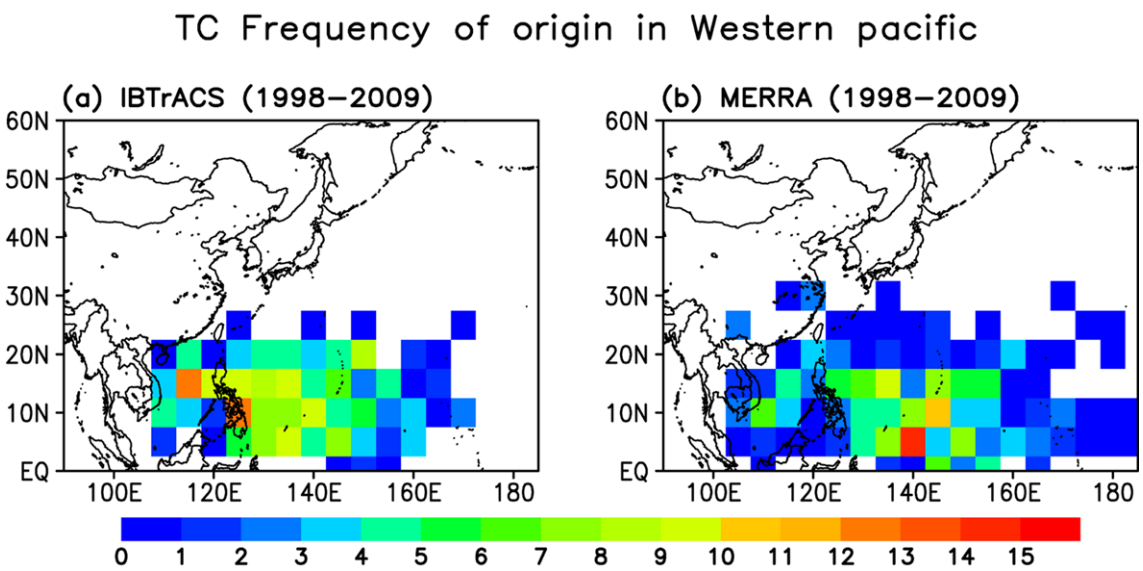

Fig. 3. The total number of tropical storms generated in each 5° latitude by 5° longitude grid box in (a) IBTrACS and (b) MERRA.

the oceanic area of 110-170°E and 5-30°N, where the main development regions are the South China Sea and the Northwestern Pacific to the east of the Philippines. In general, MERRA captures these main development regions, although the simulated locations are more widespread. Unlike the observations, a few storms are found over the inland area in China in MERRA, as the detection algorithm does not discriminate whether the genesis point is located over land or ocean in this study.

In MERRA, more storms are detected over the deep tropics (0-10°N) along the 130-170°E longitudes compared with the observations, where as MERRA generates relatively less storms over the South China Sea. This discrepancy is better illustrated in Fig. 3, where the genesis frequency (defined as the total number of storms per decade) is calculated for each 5° × 5° grid box over the domain. Over the Pacific, the main development region in MERRA tends to be shifted to the south and to the

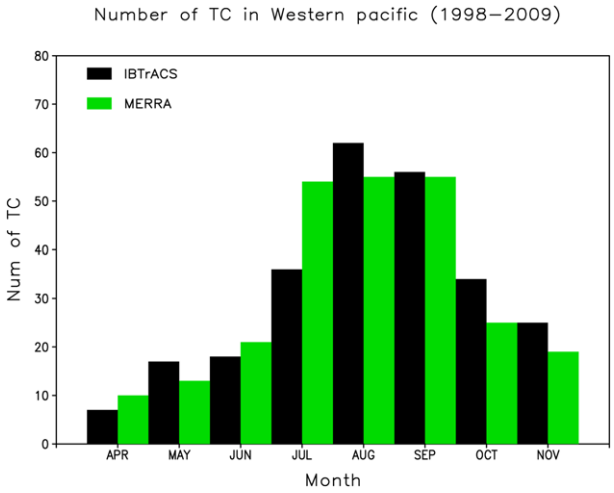

Fig. 4. Monthly variation of the number of tropical storms generated total for 12 years (1998-2009). The black bar indicates IBTrACS and the green bar indicates MERRA.

east compared with the observed center in IBTrACS. Note that this is more or less caused by the difference in the storm detection between the observation and the reanalysis. As illustrated in Figs. 1c and 1d, the detection algorithm tends to begin tracking earlier than the observed, whereas the IBTrACS observation is not reported until the storm develops into a tropical depression. This might increase the population of tropical storm genesis on the upstream side along the major tropical storm path. In this regard, a careful examination of the genesis points in MERRA should provide some useful information on the initiation process of tropical storms.

Figure 4 compares the seasonal cycle of tropical storm genesis, where we indicate the monthly number of the total storms developed for the past 12 years in IBTrACS and MERRA. MERRA shows a reasonable seasonal variation, and the correlation with the observed time series is over 0.95. However, the reanalysis shows too many storms developing in July, which makes the variation rather flat during the peak season. We note that this is rather sensitive to the detection criteria - we obtained a more realistic peak in August when we applied a loosened criterion in the storm detection (the 0.5 standard deviation in the warm-core detection) and increased the number of sampled storms.

c. Track

Once developed, the tropical storms simulated by MERRA exhibit reasonable migration paths toward higher latitudes. Figures 5a and 5b show the observed and simulated tracks from IBTrACS and MERRA, respectively. Observed tracks are the superposition of various storm paths, which are by and large grouped into the two major paths over the basin: 1) the westward or northwestward paths in a relatively straight line

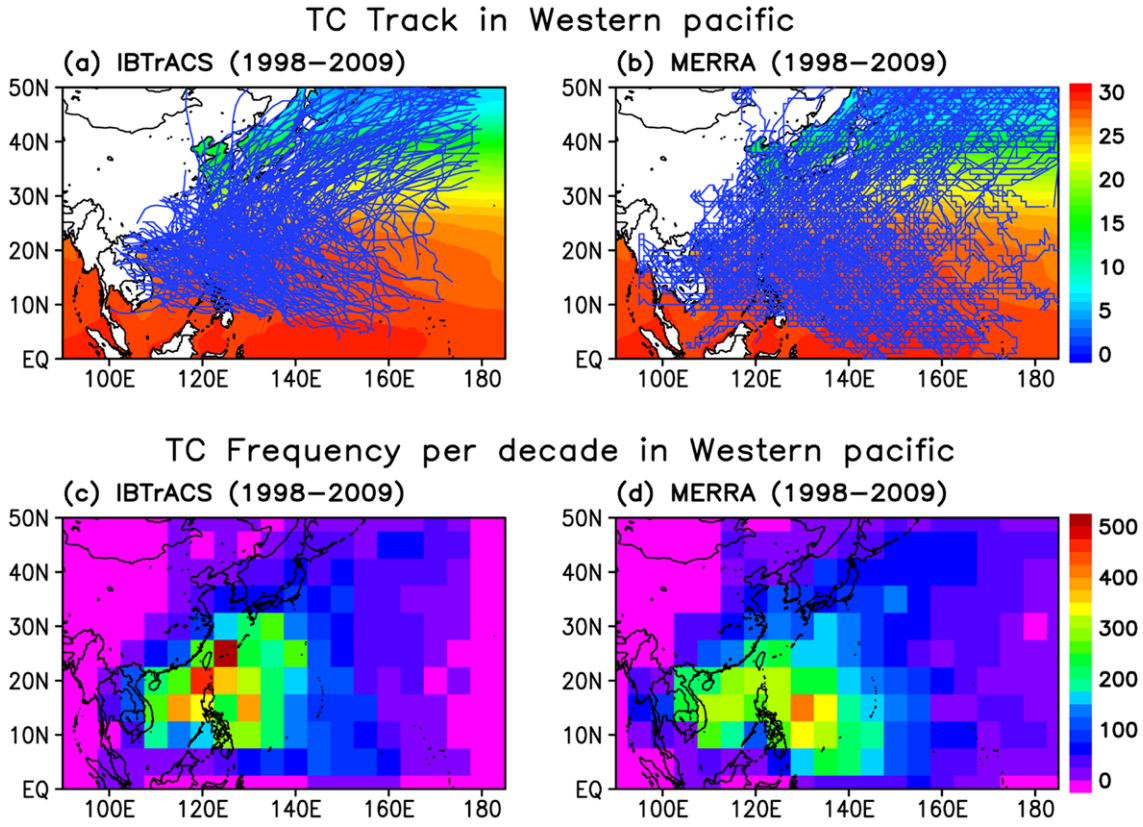

Fig. 5. (a) Tropical storm tracks in the observation and (b) the reanalysis. (c) and (d) are the number frequency of the storm track per decade from the observation and the reanalysis, respectively. Note that the observation finishes reporting at the International Dateline (180°E).

from the genesis region, affecting the Philippines, southern China, Taiwan, and Vietnam, and 2) the curved paths initially westward or northwestward from the genesis region, and then turning toward the north or northeast, affecting eastern China, Taiwan, Korea, and Japan. In general, the MERRA simulation captures these migrating features reasonably well. Recurving latitudes of the curved paths are between 20-30°N in both the observations and the reanalysis. However, MERRA shows a lot of tracks in the deep tropics below 10°N and 140-160°E, presumably due to the relatively earlier detection of tropical storms on the upstream side (results that are consistent with Figs. 2 and 3).

For a quantitative analysis of the path frequency, we calculated the track density for each $5^{\circ} \times 5^{\circ}$ grid box and present the results in Figs. 5c and 5d. The observations (Fig. 5c) shows an "arrow-head" pattern with frequent paths along the South China Sea and the western Pacific near the Philippines, which are connected just east of Taiwan. The reanalysis (Fig. 5d) tends to capture this arrow-head pattern, although the track density is relatively higher in the western Pacific than in the South China Sea. It is not clear whether the relatively small density of the tracks in MERRA over the South China Sea is related to the weaker tropical storm genesis (Fig. 3b), since this requires a systematic decomposition of tracks according to the genesis location. Clustering of the observed and the simulated paths seem to be useful in this regard, as studied in Kim *et al.* (2011), and this is left for future study.

d. Maximum intensity

This section compares the maximum intensity of tropical storms in IBTrACS and MERRA, as represented by the minimum center pressure and the maximum surface wind speed at their full development. By examining the entire life time of each storm, we obtained the lowest value of the center pressure and the highest wind speed. This is shown in Fig. 6 as a scatter plot between these two variables. In the reanalysis, the time at which the storm reaches its minimum sea level pressure and maximum wind speed is not necessarily same, although the times are very close.

In order to understand the difference between the observations and the reanalysis, the definition of the maximum sustained wind speed in the tropical storm observations must be clarified. The maximum sustained wind speed is commonly used to categorize the tropical storm by intensity. The widely used definition of sustained winds among most agencies is that of a 10 minute average at a height of 10 m. IBTrACS is a merged product from different sources of tropical storm observations, mostly archived by the RSMC in Tokyo and the US Joint Typhoon Warning Center (JTWC) in the northwest Pacific basin. The definition of the maximum sustained wind is slightly different between these two agencies. RSMC Tokyo uses 10 minute average winds, whereas the US Joint Typhoon Warning Center defines the sustained wind based on a 1-minute average wind speed, which is converted to a ten-minute value by multiplying by 0.88 (Knapp and Kruk, 2010). According to the

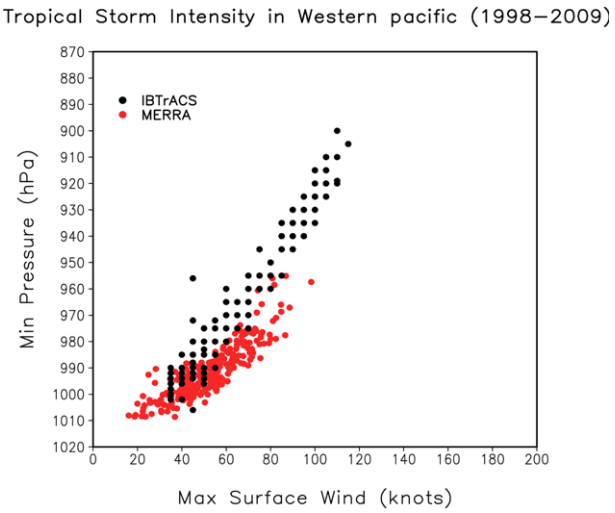

Fig. 6. Comparison of the maximum intensity of the tropical storms represented with the maximum surface wind speed (unit: knots) and the minimum sea level pressure (hPa) at their maximum development phases. The observation is indicated as black dots and the reanalysis is indicated as red dots. For the reanalysis, only the tropical storms lasted for more than a day are shown. The wind speed in IBTrACS is the observed maximum sustained wind speed at 10 m, whereas the reanalysis uses the wind speed at 925 hPa, which is the lowest pressure level data in the output.

RSMC classification, four different categories of wind speed are used to measure the intensity of a tropical storm. A tropical depression is the lowest category for a tropical system that has wind speeds not exceeding 35 knots - these are not included in this study. The second lowest category is the tropical storm with sustained wind speeds exceeding 35 knots. More intensive storms that reach sustained wind speeds of 50 knots are classified as severe tropical storms, and the storms reaching wind speeds of 65 knots are designated as tropical cyclones (typhoons)-the highest category.

For the observed tropical storms, the scatter plot shows a linear relationship between the minimum sea level pressure and the maximum sustained wind speed at 10 m, with a slope of about 1.2 hPa deepening per knot. The observed maximum wind speeds are all above 35 knots, because the tropical depressions that never reach tropical storm intensity (> 34 knots) are excluded from this study. The wind speed is reported in a 5 knot interval after this threshold value (35 knots). The observed maximum wind speed increases up to 115 knots, which is the strongest tropical storm in the past 12 years. Most of the observed storms are concentrated in the second category of the RSMC classification (the tropical storm), and then widely spread over the categories of severe tropical storm and tropical cyclone (typhoon).

The reanalysis also tends to capture the proportional relationship between the minimum pressure at the storm center and the maximum surface wind speed, although the deepening rate of the center pressure per unit wind speed increase is smaller when compared with the observations. Note that the wind speed at 925 hPa was used for the reanalysis as a substitute for the 10-m

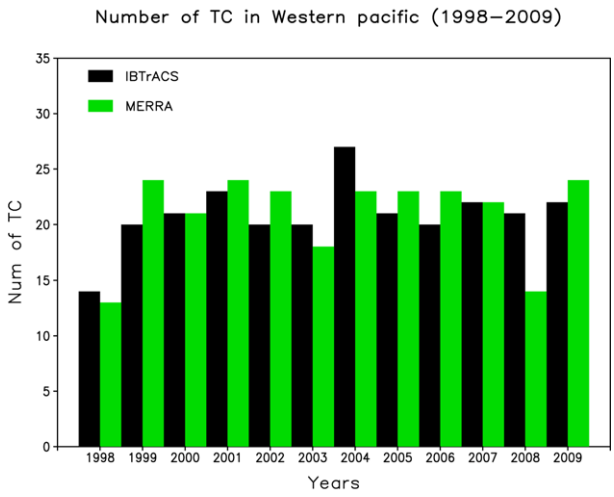

Fig. 7. Year-to-year variations of the tropical storm genesis in IBTrACS (black), and MERRA (green) for the period of 1998-2009.

surface wind. Although MERRA originally provides 10 m winds, this is a 1-hour average and it considerably underestimates the wind speed at the storm center. Instead, we use instantaneous values for the sea level pressure and the 925 hPa wind obtained from the data assimilation with the 20 minute time step, and the resulting magnitude compares better with the tropical storm observations. The primary deficiency in MERRA is the inability to simulate severe storms, partly due to the horizontal resolution (~ 50 km) of the global model, and partly due to the deficiency in the parameterized deep convection. Although the most intense storm in the model has maximum surface wind speeds over 100 knots, its center pressure remains above 950 hPa, so that the reanalysis significantly underestimates storm deepening.

e. Interannual variation

Figure 7 shows the interannual variation of tropical storm genesis in the observations and MERRA. MERRA tends to reproduce the observed interannual variation of the number of tropical storms developed, but with the limited accuracy (the correlation between the observed and the reanalysis time series is below 0.6). As discussed in Section 2b, the correlation coefficient becomes slightly higher (0.65) when we apply the warm-core temperature threshold with the 0.5 standard deviation in the detection algorithm, but this seems to be only a marginal improvement. Of course, 12 years provide only a very limited sample, and this should be validated with longer-term statistics. On the other hand, a careful examination of the cases of specific years might be helpful in diagnosing problems with the reanalysis. For example, the least active year of 1998 in the IBTrACS observation is reasonably well captured by MERRA. However, MERRA underestimates the number of storms in the most active year (2004), regardless of the detection threshold change, and it also substantially underestimates the storm count in 2008.

4. Summary and conclusions

This study examined the representation of tropical storms in the Northwest Pacific during the past 12 years (1998-2009) in the new MERRA atmospheric reanalysis. For comparison, the observed best track dataset for tropical storms from IBTrACS was analyzed for the same period. The detection and tracking algorithm originally developed by Camargo and Zebiak (2002) was used to detect the tropical storms in the reanalysis. This method relies on basin-dependent threshold criteria for three atmospheric variables, consisting of the relative vorticity at 850 hPa, the wind speed at 10 m above the surface, and the vertically-integrated temperature anomaly at the storm center.

Compared with the IBTrACS observation, the main development regions of tropical storms in the northwest Pacific basin are reasonably well captured in MERRA by resolving the two dominant areas of development in the South China Sea and the Northwest Pacific to the east of the Philippines. However, the reanalysis genesis locations tend to be more widespread, and the reanalysis tends to develop more storms in the deep tropics, on the upstream side of the major storm tracks. As a result, the main development region is shifted to the south and toward the east over the Northwest Pacific in the reanalysis, thereby undercounting storms in the subtropics and in the South China Sea, and overcounting storms in the tropical oceans equatorward of 5°N. The seasonal cycle of tropical storm genesis is reasonable in MERRA, with maximum values during July to September and the minimum in April. Also, MERRA reproduces the observed interannual variation in the yearly number of tropical storms developed, but with lower correlation with observations than for the seasonal variation.

The simulated tropical storm tracks in MERRA also show reasonable agreement with the observational data. The model resolves the two most frequent types of storm tracks, one that is westward or northwestward in a relatively straight line from the storm origin, affecting South Asia and the southern China, and another with curved paths that are initially northwestward from the origin and then turning toward the northeast between latitudes 20-30°N, and affecting eastern China, Korea, and Japan. However, the reanalysis has a relatively weaker signal in the track density over the South China, along with the less development over this region compared with the observations. It is not clear whether the relatively smaller density of the tracks in MERRA over the South China Sea is related to the weaker tropical storm genesis in the model, and this requires a systematic decomposition of tracks according to the genesis location, which is left for future study.

Regarding the maximum intensity of the tropical storms detected, the reanalysis tends to capture the relationship between the minimum sea level pressure at the storm center and the maximum surface wind speed. However, the deepening rate of the center pressure per unit surface wind increase is smaller than in the observations. This deficiency is also reflected in the inability to produce the most intense storms. The model significantly underestimates the deepening of center pressure and

the surface wind speed, even though the wind speed comparison between the observation and the reanalysis is not straightforward. It is suggested that this is in part due to the coarse horizontal resolution (~ 50 km) of the global model used in the reanalysis, and in part due to deficiencies in the parameterized deep convection.

The major findings of this study highlight two important scientific implications. First, MERRA is capable of resolving the long-term climatology of weather extremes - in particular tropical storms. Despite some deficiencies in MERRA, the climatological-mean behavior of the genesis locations, tracks, and the intensity of tropical storms are reasonably well reproduced in the data assimilation mode. This is presumably a result of global model improvements and the increased horizontal resolution of the data assimilation system. Considering that tropical storms are one of the important and efficient processes for transferring heat and moisture toward higher latitudes, one can expect improved energy and water cycles in MERRA compared with earlier reanalyses. Other extreme weather events such as extra-tropical storms and persistent droughts should be further validated in this regard.

Second, the simulation of tropical storms in data assimilation mode should provide useful guidance for improving dynamical prediction systems based on general circulation models. The results can, for example, be compared with free running model simulations, using the same model that was used in the reanalysis but without observational data constraints. Such an investigation should provide useful information for discriminating between differences in large-scale forcings and the triggering and maintaining mechanisms of tropical storms.

Acknowledgements. We thank Dr. Lindsey Williams and Dr. Jae Schemm at NCEP CPC for providing the source code of the tropical storm detection and tracking algorithm. We are also thankful to Dr. Jong-Seong Kug and an anonymous reviewer for their valuable comments on the first draft. This work was funded by the Korea Meteorological Administration Research and Development Program under Grant RACS_2010-2004 in 2010. This study was also supported by NASA's Modeling, Analysis, and Prediction (MAP) program.

REFERENCES

Bosilovich, M. G., J. Chen, F. R. Robertson, and R. F. Adler, 2008: Evaluation of Global Precipitation in Reanalyses. *J. Appl. Meteor. Climatol.*, **47**, 2279-2299.

Bloom, S., L. Takacs, A. DaSilva, and D. Ledvina, 1996: Data assimilation using incremental analysis updates. *Mon. Wea. Rev.,* **124**, 1256-1271.

Bosilovich, M. G., F. R. Robertson, and J. Chen, 2011: Energy and water budgets in MERRA. *J. Climate*, Submitted.

Camargo, S. J., and S. E. Zebiak, 2002: Improving the detection and tracking of tropical cyclones in atmospheric general circulation models. *Wea. Forecasting*, **17**, 1152-1162.

Chou, M. -D., and M. J. Suarez, 1999: A Solar Radiation Parameterization for Atmospheric Studies. NASA Technical Report Series on Global Modeling and Data Assimilation 104606, **15**, 40 pp.

_____, M. J. Suarez, X. Z. Liang, and M. M.-H. Yan, 2001: A Thermal Infrared Radiation Parameterization for Atmospheric Studies. NASA Technical Report Series on Global Modeling and Data Assimilation 104606, **19**, 56 pp

Garcia, R. R. and B. A. Boville, 1994: Downward control of the mean meridional circulation and temperature distribution of the polar winter stratosphere, *J. Atmos. Sci.,* **51**, 2238-2245.

Kalnay, E., and Coauthors, 1996: The NCEP/NCAR 40-Year Reanalysis Project. *Bull. Amer. Meteor. Soc.*, **77**, 437-471.

Kanamitsu, M., W. Ebisuzaki, J. Woolen, S.-K. Yang, J. J. Hnilo, M. Fiorino, and G. L. Potter, 2002: NCEP-DOE AMIP-II Reanalysis (R-2). *Bull. Amer. Meteor. Soc.,* **83**, 1631-1643.

Kim, H.-S., J.-H. Kim, C.-H. Ho, and P.-S. Chu, 2011: Pattern classification of typhoon tracks using the fuzzy c-means clustering method, *J. Climate*, **24**, 488-508.

Knapp, K. R. and M. C. Kruk, 2010: Quantifying interagency differences in tropical cyclone best-track wind speed estimates, *Mon. Wea. Rev.*, **138**, 1459-1473.

_____, _____, D. H. Levinson, H. J. Diamond, and C. J. Neumann, 2010: The International Best Track Archive for Climate Stewardship (IBTrACS): Unifying tropical cyclone best track data. *Bull. Amer. Meteor. Soc.*, **91**, 363-376.

Koster, R. D., M. J. Suárez, A. Ducharne, M. Stieglitz, and P. Kumar, 2000: A catchment-based approach to modeling land surface processes in a GCM, Part 1, Model Structure. *J. Geophys. Res.*, **105**, 24809-24822.

Lin, S.-J., 2004: A vertically Lagrangian finite-volume dynamical core for global models. *Mon. Wea. Rev.,* **132**, 2293-2307.

Lock, A. P., A. R. Brown, M. R. Bush, G. M. Martin, and R. N. B. Smith, 2000: A new boundary layer mixing scheme. Part I: Scheme description and single-column model tests. *Mon. Wea. Rev.,* **138**, 3187-3199.

Louis, J., M. Tiedtke, and J. Geleyn, 1982: A short history of the PBL parameterization at ECMWF. *Proc. ECMWF Workshop on Planetary Boundary Layer Parameterization*, Reading, United Kingdom, ECMWF, 59-80.

McFarlane, N. A., 1987: The effect of orographically excited gravity wave drag on the general circulation of the lower stratosphere and troposphere. *J. Atmos. Sci.,* **44**, 1775-1800.

Moorthi, S., and M. J. Suarez, 1992: Relaxed Arakawa-Schubert, A Parameterization of Moist Convection for General-Circulation Models. *Mon. Wea. Rev.* **120**, 978-1002.

Onogi, K., and Coauthors, 2007: The JRA-25 Reanalysis. *J. Meteor. Soc. Japan*, **85**, 369-432.

Rienecker, M. M., and Coauthors, 2008: The GEOS-5 Data Assimilation System - Documentation of Versions 5.0.1, 5.1.0, and 5.2.0. NASA Tech. Rep. Series on Global Modeling and Data Assimilation Vol. 27, 101 pp.

_____, and Coauthors, 2011: MERRA - NASA's Modern-Era Retrospective Analysis for Research and Applications, *J. Climate*, Submitted.

Saha, S., and Coauthors, 2010: The NCEP Climate Forecast System Reanalysis. *Bull. Amer. Meteor. Soc.*, **91**, 1015-1057.

Uppala, S., and Coauthors, 2005: The ERA-40 Re-Analysis. *Quart. J. Roy. Meteor. Soc.*, **131**, 2961-3012.

Wu, W.-S., R. J. Purser, and D. F. Parrish, 2002: Three-dimensional variational analysis with spatially inhomogeneous covariances. *Mon. Wea. Rev.*, **130**, 2905-2916.